Modeling effect of time delay for large network of seismic monitor

Jordi Anguera[*] Leevi Annala[†] Stefan Dimitrijevic[‡]
Patricia Pauli[§] Liisa-Ida Sorsa[¶] Dimitar Trendafilov[‖]
Christophe Pickard[**]

17.7.2018

Abstract

1 Introduction

The purpose of this work is to analyze noise in a large network of seismic monitors and to extract clock drift from the noise. Constant GPS synchronization of data is not possible due to the high energy consumption. This work suggests an alternative way to determine clock drift based on the data only.

2 Assumptions

All the stations have the same orientation. The medium the wave is propagating in is homogenous.

[*]Autonomous University of Barcelona, Spain
[†]University of Jyväskylä, Finland
[‡]University of Novi Sad, Serbia
[§]Technical University of Darmstadt, Germany
[¶]Tampere University of Technology, Finland
[‖]University of Sofia "St. Kliment Ohridski", Bulgaria
[**]University of Grenoble Alpes and Grenoble INP, France

3 Data

The data is collected from a network of 73 seismic monitor stations recording ground vibrations in the Southeast region of France. The GPS coordinate position of each station in the network is known (Figure 1) and they each contain a clock which is synchronized to the GPS once a month. The seismic monitor sensor records compression and decompression as discrete values -1 and 1, respectively, every second. The sensor responds to any event in the area, be it an earthquake, tremor from road traffic, airplane or any other pressure wave which travels in the ground.

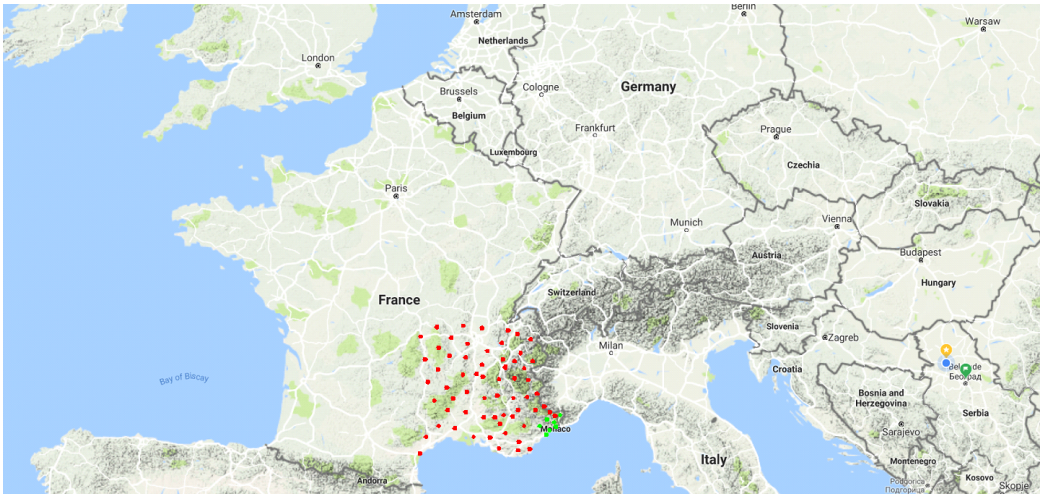

Figure 1: The network of seismic monitors are located in the Southeast France, mostly in the regions of Provence-Alpes-Côte d'Azur and Rhône-Alpes. The seven stations chosen as the small test set is shown as green in the southeast part of the area.

The stations work independent of each other and are occasionally shut down for some time frame for maintenance, repair or just random events. Just as occasionally they are brought up to measure again. Therefore, the number of active stations varies over time. The Figure 3(a) shows the number of working stations, and the Figure 3(b) the number of working connections between the monitor stations over one year of measurements.

The compression and decompression data recorded by the stations is retrieved and run through initial data cleaning and filtering procedures. The data is then cross-correlated in one-hour time windows to yield time-delay data of signal between each monitor (Figure 3).

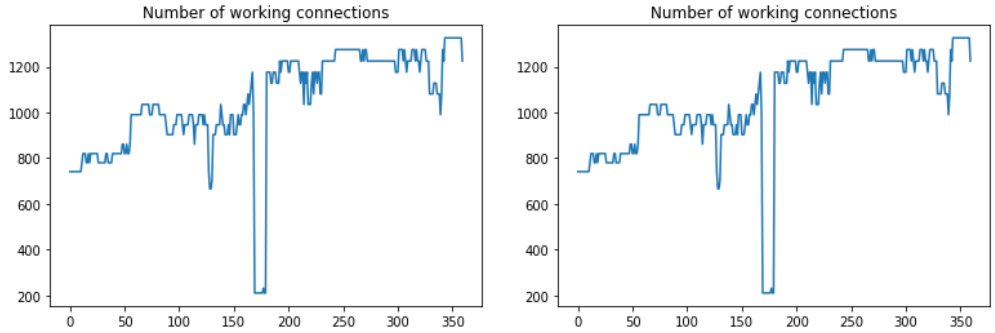

(a) The number of working seismic monitor stations.

(b) The number of working connections between the stations.

Figure 2: Working stations and connections over one year time period. !!!TODO: update figures here

The time delays between each monitor are assumed to depend on the distance between the monitor. The further away the monitors are from each other, the larger the time delay caused by the same event recorded by the monitor. The Figure 4 shows an example of time-delay evolution of one monitor station over 24 hours. The distributions are symmetric because each monitor connection is computed into both directions. The interesting feature of the histograms is how the shape of the distribution changes.

The figure 4 shows clearly how the time delays change over time. However, the mean remains zero.

4 Methods

4.1 Modelling time delay between seismic monitors

The network of monitors can be modelled as a complete graph. The signal of each monitor is cross-correlated with other monitor signals, finally yielding time-delay data between each monitor. The time delay between the monitors comprise information on the real time the signal travels between the monitors, the inaccuracies of the clock (time drift), and other noise affecting the measurement.

Let $\hat{\boldsymbol{\delta}} \in \mathbb{R}^{n \times n}$ be the measured pairwise time delays of the system, $\boldsymbol{\delta}$ the actual pairwise time delays, and $\boldsymbol{\varepsilon}$ an error term including clock drift of the station's clock and other errors

$$\hat{\boldsymbol{\delta}} = \boldsymbol{\delta} + \boldsymbol{\varepsilon}. \tag{1}$$

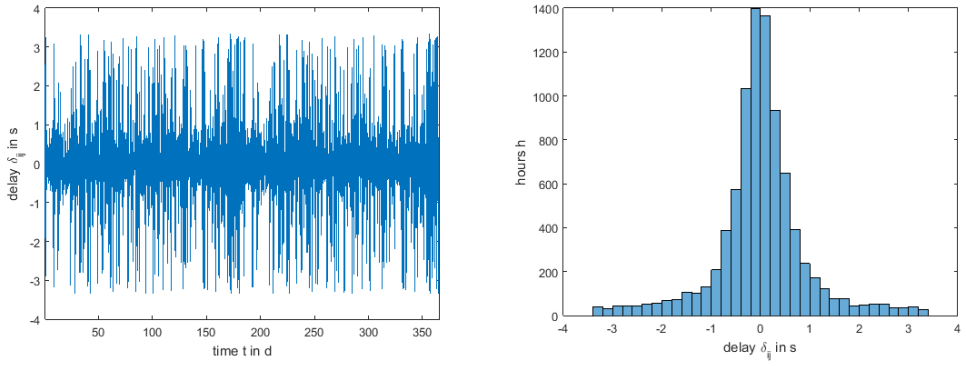

(a) Time Signal. (b) Histogram.

Figure 3: The time-delay signal recorded between one station pair over a year. The time delay is computed in one-hour windows, yielding 24 time-delay values over a day.

Each of the monitors are equipped with a clock which runs independent of others. It is synchronized via GPS system once a month and then runs independently. The drift, ε_i in clock i is caused by variation in the clocks oscillator.

The position of each seismic monitor in the network is known. As the monitors are spread across a large area, it is assumed that local tremors are detected by stations that are close by, and therefore the correlations found in the pairwise cross-correlations and time delay data between them have higher likelihood to be linked.

4.2 Denoising model

4.2.1 Definitions

The computational denoising model involves weighted network estimation by the use of topological graph metrics, described in detail in [2].

We have a weighted graph $\mathcal{G} = (\mathcal{V}, \mathcal{E}, \hat{\delta}_{\mathbf{t}})$ defined by a finite set of nodes $\mathcal{V}$ with $|\mathcal{V}| = n$, a set of edges $\mathcal{E} = \{(v_i, v_j) \in \mathcal{E}\}$, with $|\mathcal{E}| = n^2 - n$ and the weighted adjacency matrix $\hat{\boldsymbol{\delta}}$ with $\delta_{ii} = 0$ for all i. The matrix $\hat{\boldsymbol{\delta}}$ is symmetric and describes the time delays between events in the graph, and is normalized, i.e. $\hat{\delta}_{ij} \in [0, 1]$. The adjacency matrix indicates the strength of connection between nodes. Therefore, the shorter the time delay between nodes, the stronger the connection, and higher the value.

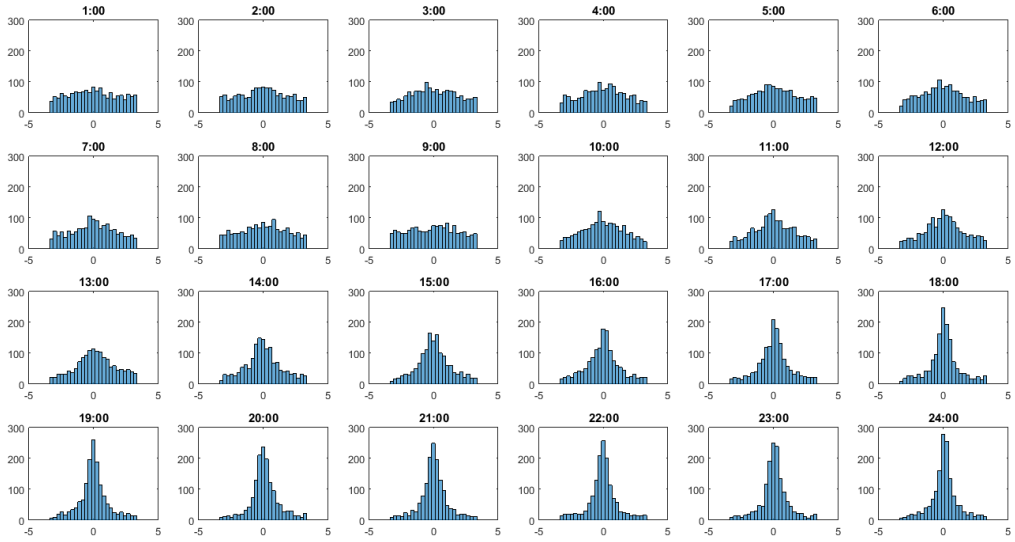

Figure 4: Histograms of time delays of all active stations recorded over 24 hours. The histogram shows how many connections have a particular delay at the instant.

4.2.2 Cost function

We assume to have estimates of M differentiable graph metrics of the original matrix $\boldsymbol{\delta}$, i.e. $f_m(\boldsymbol{\delta}) = K_m$, where $m \in \{1, \ldots, M\}$, then we can formulate a cost function that measures the deviation of the observed weight matrix's metrics $f_m(\hat{\boldsymbol{\delta}})$ to the estimates K_m as:

$$c(\hat{\boldsymbol{\delta}}) = \sum_m e_m^2(\hat{\boldsymbol{\delta}}) = \sum_m (f_m(\hat{\boldsymbol{\delta}}) - K_m)^2 \tag{2}$$

The error is minimized with gradient descent updates on $\hat{\boldsymbol{\delta}}$:

$$\hat{\boldsymbol{\delta}}^{(t+1)} = \hat{\boldsymbol{\delta}}^t - \mu \sum_m e_m(\hat{\boldsymbol{\delta}}^t) \frac{df_m(\hat{\boldsymbol{\delta}}^t)}{d\hat{\boldsymbol{\delta}}^t}, \tag{3}$$

where t is the iteration index and μ the learning rate. For the case of $m = 1$, Equation 3 describes the traditional single function gradient descent.

4.2.3 Graph metrics

Graph metrics are scalar functions of the weight matrix, $f(\hat{\boldsymbol{\delta}}) : \mathbb{R}^{n \times n} \to \mathbb{R}$. We choose graph metrics to:

1. **Distance**: We want to use the distance measures to denoise the delay measurements. For this purpose, we deisigned a metric, the connection strength of a node i. We normalize the delays and compute the row sum

$$f_i(\boldsymbol{\delta}) = \sum_j \delta_{ij}. \tag{4}$$

Thde connection strength can be interpreted as the sum of all normalized delays of all of the links to node i.

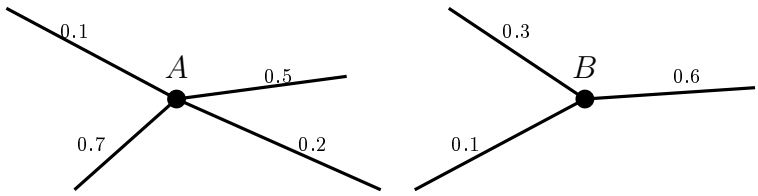

Figure 5: Distance metric.

Figure 5 shows two nodes. Node A has four connections yielding a connection strength $0.1+0.5+0.7+0.6 = 1.9$ whereas node B only has three connections. Thus, the connection strength is $0.3+0.6+0.1 = 1$.

The constants K_m are defined as follows

$$K_m = f_m(\boldsymbol{W}_d) \tag{5}$$

It is the connection strength as well. But now we plug in the distance matrix $\boldsymbol{W_d}$. The distances are constants and yield a constant K_m. The weight matrix $\boldsymbol{W_d}$ is a function of the distance between node i and node j. First, we choose the function to be the reciprocal of the distances of the node to all other nodes, $d_{ij} = 1/r_{ij}$, normalized between $[0, 1]$. Higher values correspond to nodes with short distances to all other nodes. Second, we try a metric with weights proportional to the distances, normailzed between $[0, 1]$ accordingly. Here, high values correspond to long distances between two stations.

We find the derivative for the gradient descent update step.

$$\frac{df_2}{d\boldsymbol{\delta}} = \frac{\sum_j \delta_{ij}}{d\boldsymbol{\delta}} = \begin{bmatrix} 0 & 1 & 0 & \dots & 0 \\ 1 & 0 & 1 & \dots & 1 \\ 0 & 1 & 0 & \dots & 1 \\ \vdots & \vdots & \vdots & \ddots & \vdots \\ 0 & 1 & 0 & \dots & 0 \end{bmatrix} \tag{6}$$

It is a symmetric matrix with ones in the ith row and ith column. The diagonal entries remain zero.

We expect the following correlation between the distance of two stations and the delay between them. The further apart the stations, the greater is the delay. Figure 6 shows that the variance of the delays is much higher for a station pair of stations that are far apart.

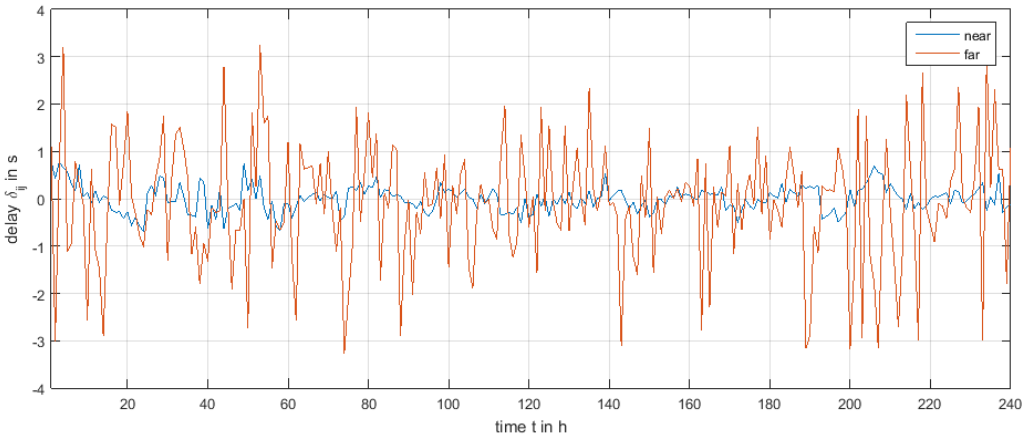

Figure 6: Comparison of the delay of the furthest and closest station pairs over 10 days.

2. Average neighbour degree, resilience:

   The average neighbour degree for node i is given by

4.3 Clock drift estimate

The denoising model in section 4.2 computes the denoised estimate of the measurement data $\hat{\boldsymbol{\delta}}$. The algorithm is run over a series of time points and an estimate for the clock drift between each station pair is obtained.

A polynomial fitting algorithm !!!TODO: specify is run to find an estimate for the trend in noise. The error term in the fitting procedure will account for all the other errors in the system. The trend is considered to be caused by the clock drifts of the two stations.

The noise, ε_{ij}, between each pair between two stations in the system is modelled with

$$\varepsilon_{ij} = |\Delta_i - \Delta_j| + e_{ij}, \tag{7}$$

in which $|\Delta_i - \Delta_j|$ is the clock drift between two stations i and j, and e_{ij} accounts for all other noise in the system in addition to the clock drift.

The clock errors of individual stations can be written in matrix form

$$\begin{bmatrix} 1 & -1 & 0 & 0 & \dots & 0 & 0 \\ 1 & 0 & -1 & 0 & \dots & 0 & 0 \\ 1 & 0 & 0 & 0 & \dots & 0 & 0 \\ \vdots & \vdots & \vdots & \vdots & \ddots & \vdots & \vdots \\ 1 & 0 & 0 & 0 & \dots & 0 & -1 \\ -1 & 1 & 0 & 0 & \dots & 0 & 0 \\ 0 & 1 & -1 & 0 & \dots & 0 & 0 \\ \dots & \dots & \dots & \dots & \dots & \dots & \dots \\ 0 & 0 & 0 & \dots & 0 & 1 & -1 \end{bmatrix} \begin{bmatrix} \Delta_1 \\ \Delta_2 \\ \Delta_3 \\ \vdots \\ \Delta_{n-1} \\ \Delta_n \end{bmatrix} = \begin{bmatrix} \Delta_1 - \Delta_2 \\ \Delta_1 - \Delta_3 \\ \vdots \\ \Delta_1 - \Delta_n \\ \Delta_2 - \Delta_1 \\ \Delta_2 - \Delta_3 \\ \vdots \\ \Delta_{n-1} - \Delta_n \end{bmatrix} = \begin{bmatrix} \Delta_{12} \\ \Delta_{13} \\ \vdots \\ \Delta_{1n} \\ \Delta_{21} \\ \Delta_{23} \\ \vdots \\ \Delta_{(n-1)n} \end{bmatrix},$$

which represents a classical overdetermined inversion problem of the form $Gm = s$, with m being the unknown model vector and s being the known data [1]. The matrix G has rank 3 because a constant offset can be added to all stations simultaneously without changing the time differences.

The matrix G is lacking full rank, therefore Tikhonov requlariza tion is employed to overcome this issue. The ordinary least squares seeks to minimize the sum of squared residuals

$$\|\mathbf{Gm} - \mathbf{s}\|_2^2. \tag{8}$$

When regularisation is added to the Equation 8, we obtain

$$\|\mathbf{Gm} - \mathbf{s}\|_2^2 + \|\mathbf{\Gamma m}\|, \tag{9}$$

for some suitable Tikhonov matrix $\mathbf{\Gamma}$. We choose this matrix as a multiple of the identity matrix $\mathbf{\Gamma} = \alpha\mathbf{I}$, giving preference to smaller norms.

The explicit solution is hence given by

$$\hat{\mathbf{s}} = (\mathbf{G}^T\mathbf{G} + \mathbf{\Gamma}^T\mathbf{\Gamma})^{-1}\mathbf{G}^T\mathbf{m}. \tag{10}$$

References

[1] C. Sens-Schonfelder. Synchronizing seismic networks with ambient noise. *Geophysical Journal International*, 174(3):966–970, 2008.

[2] L. Spyrou and J. Escudero. Weighted network estimation by the use of topological graph metrics. *CoRR*, abs/1705.00892, 2017.